NDCX-II Experimental Plans and Target Simulations

J. J. Barnard[1], R. M. More[1,2], P. A. Ni[2], A. Friedman[1], E. Henestroza[2],
I. Kaganovich[3], A. Koniges[2], J. Kwan[2], W. Liu[2], A. Ng[4],
B.G. Logan[2], E. Startsev[3] , A. Yuen[2]

1. Lawrence Livermore National Laboratory
2. Lawrence Berkeley National Laboratory
3. Princeton Plasma Physics Laboratory
4. University of British Columbia

Nineteenth International Symposium on Heavy Ion Inertial Fusion

Berkeley, CA 94720

August 12 – 17, 2012

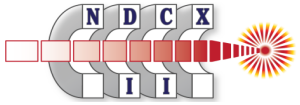

The Heavy Ion Fusion Science Virtual National Laboratory

* This work was performed under the auspices of the U.S. Department of Energy by Lawrence Livermore National Security, LLC, Lawrence Livermore National Laboratory under Contract DE-AC52-07NA27344, by LBNL under Contract DE-AC02-05CH11231, and by PPPL under Contract DE-AC02-76CH03073.

Outline of talk: NDCX-II target physics plans and simulations

1. NDCX-II physics experiments:

    - (Heavy ion fusion beam physics)

    - IFE relevant HEDLP physics

        -- Target coupling/ion driven hydrodynamics
            Rarefaction waves
            Shock waves
        -- Ion dE/dX

        -- Material properties such as conductivity

    - Target diagnostics

Original strategy: maximize uniformity and efficiency by placing center of foil at Bragg peak

In simplest example, target is a foil of solid or "foam" metal

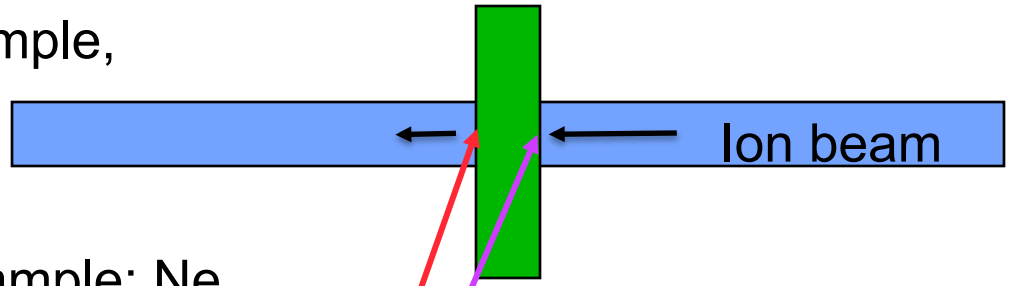

Example: Ne

Energy loss rate

$$-\frac{1}{Z^2}\frac{dE}{dX}$$

(MeV/mg cm^2)

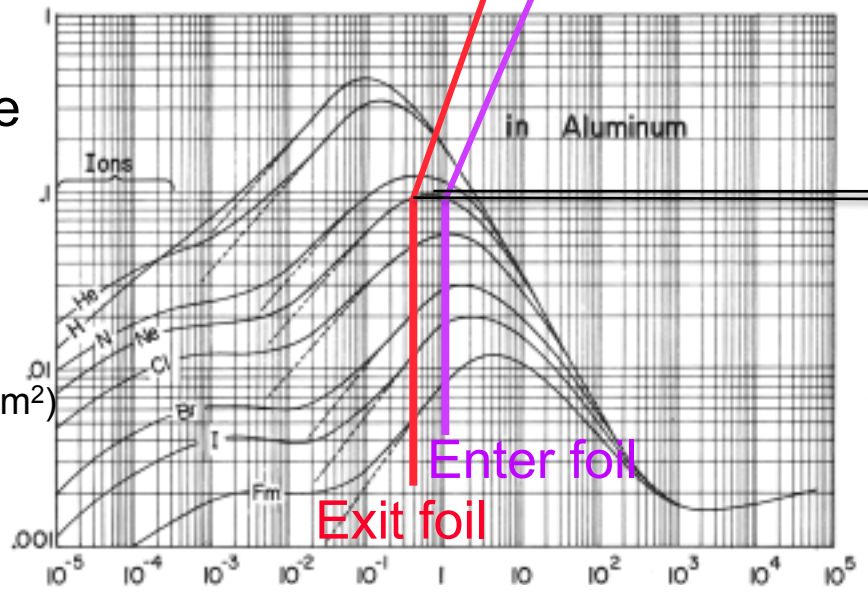

(dEdX figure from L.C Northcliffe and R.F.Schilling, Nuclear Data Tables, A7, 233 (1970))

Fractional energy loss can be high and uniformity also high if operate at Bragg peak (L. R. Grisham, Physics of Plasmas, **11**, 5727 (2004).)

$\Delta dE/dX \propto \Delta T$

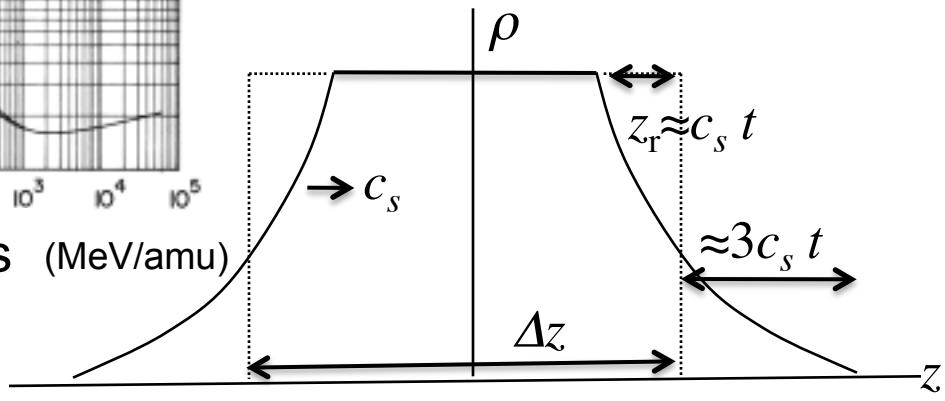

The initial configuration of NDCX-II has an ion energy of 1.2 MeV; a second stage is envisioned with an ion energy of 3.1 MeV

	Initial configuration	Stage II (~2014?)
	27 periods/12 active-cells	37 periods/21 active-cells
Ion species	Li^+: A=7	Li^+: A=7
Total charge in final pulse	30 nC	30 – 50 nC
Ion kinetic energy	1.2 MeV	3.1 MeV
Focal radius (containing 50% of beam)	0.6 mm	0.7 – 0.5 mm
Bunch duration (FWHM)	0.85 ns	0.6 – 0.2 ns
Peak current	35 A	50 – 250 A
Peak fluence (time integrated)	13 J/cm^2	~28 J/cm^2
Peak temperature	~ 1 – 2 eV	~ 2 – 3 eV
Peak pressure	0.05 – 0.2 MBar	0.2 – 0.8 MBar

* Estimates of ideal performance are from (r,z) Warp runs (no misalignments), and assume uniform 1 mA/cm^2 emission of ions, no timing or voltage jitter in acceleration pulses, no jitter in solenoid excitation, and perfect beam neutralization.

Bragg peak is at 1.9 MeV for Li on Al (so ~3 MeV desirable)
At 1.2 MeV Li is below peak for most materials

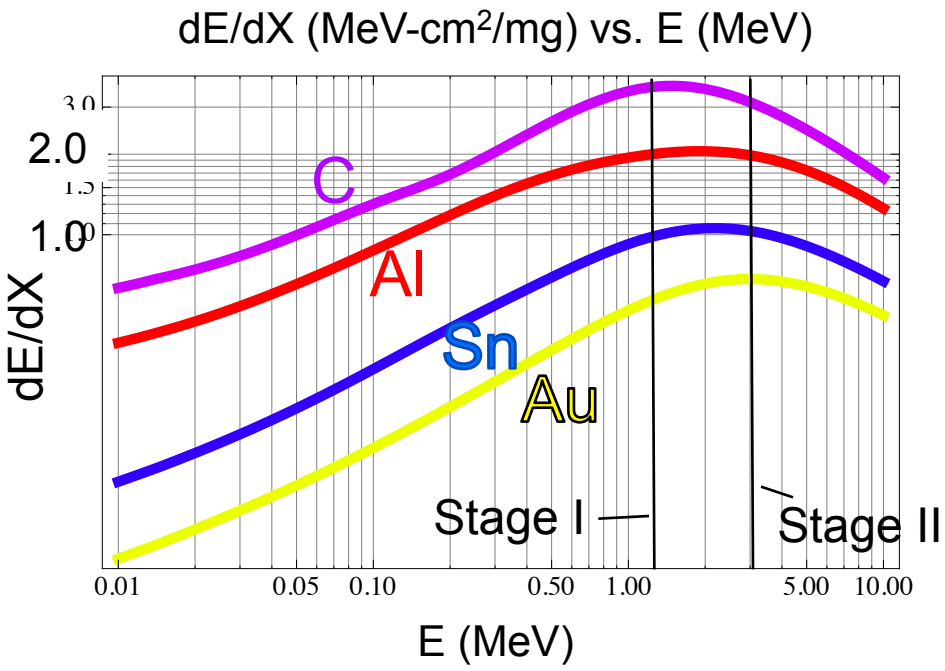

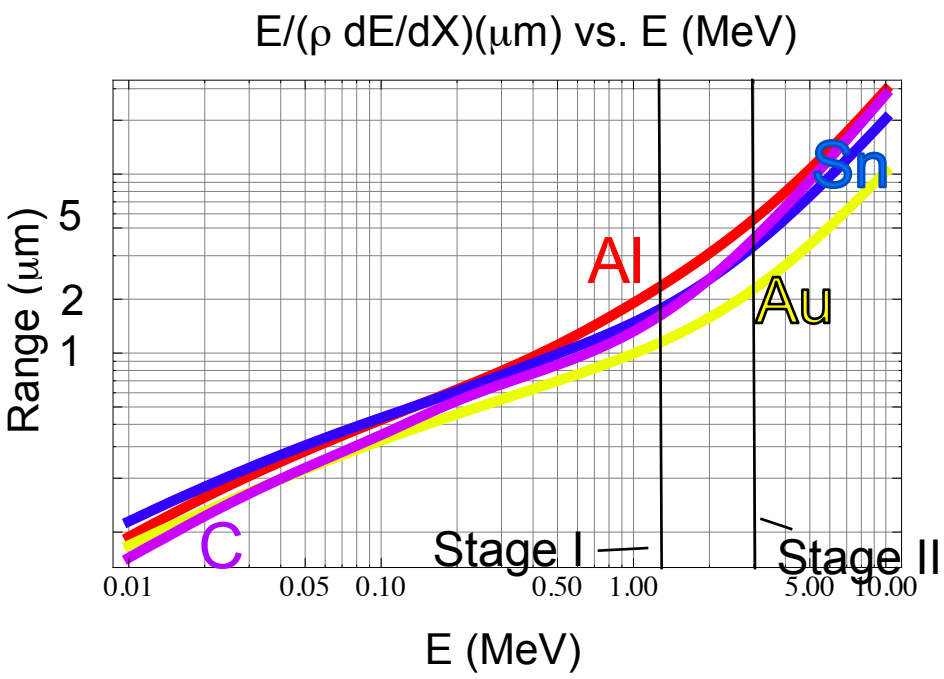

Bragg peak energies, Li on: C 1.5 MeV
Al 1.9 MeV
Sn 2.0 MeV
Au 3.0 MeV

Hydrodynamic simulations show that approximately uniform conditions can be created using Bragg peak heating (stage II)

density

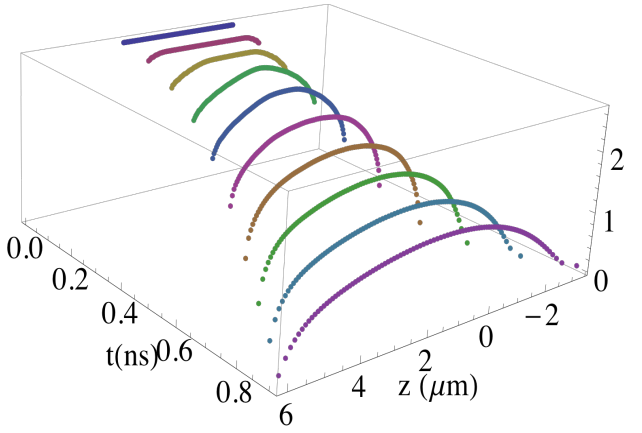

Assumed fluence:
30 J/cm^2; 2.8 MeV
Li beam on Al
target

temperature

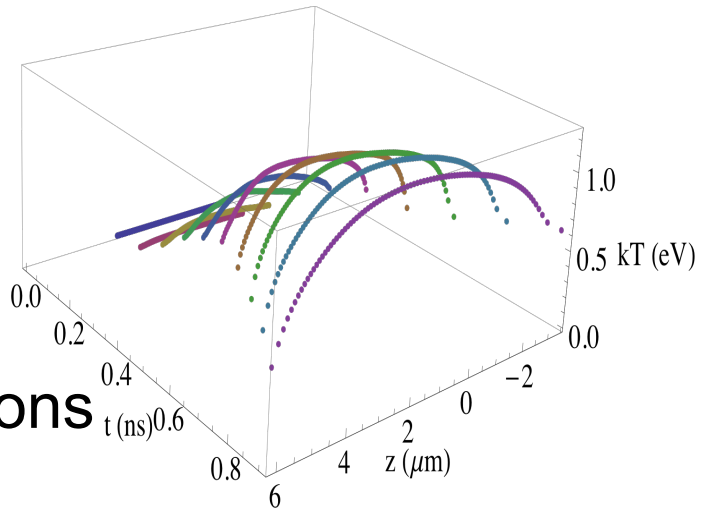

HYDRA[1] simulations

Snapshots
separated by
0.1 ns

pressure

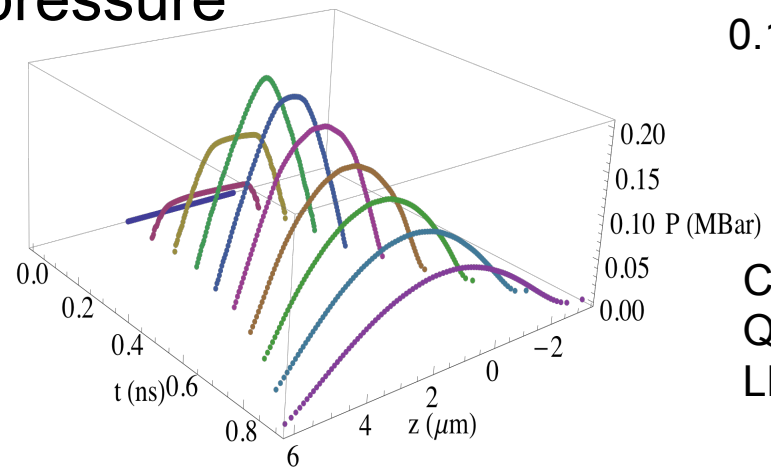

temp vs. density trajectories

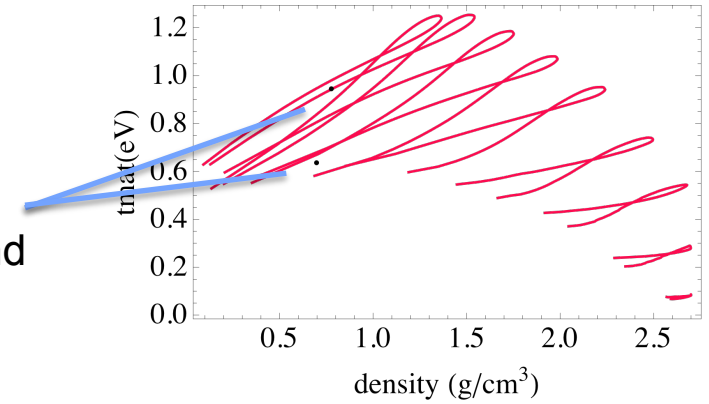

Critical points for
QEOS (upper) and
LEOS (lower)

1. M. M. Marinak et al, Phys. Plasmas **8**, 2275 (2001)

In the WDM regime, equations of state vary between models

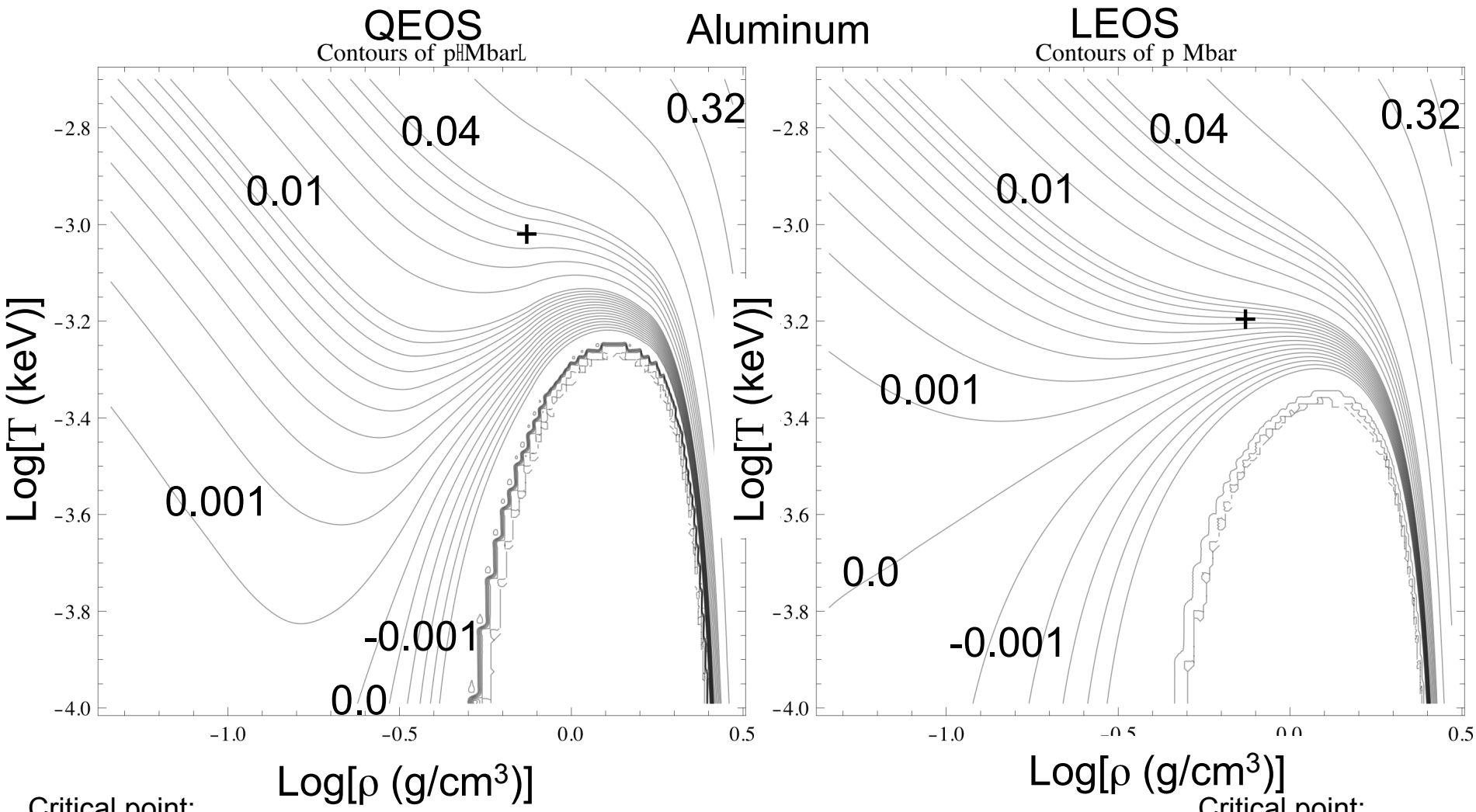

Critical point:
p=0.029 MBar
ρ=0.78 g/cm^3
T=0.945 eV

Theories and experiments place critical point between 5500 K and 12000 K (0.5 eV and 1.0 eV)

Critical point:
p=0.0065 MBar
ρ=0.70 g/cm^3
T=0.633 eV

Diagnostics for temperature, velocity and density will be compared to simulated diagnostics and depend on EOS

Pyrometry

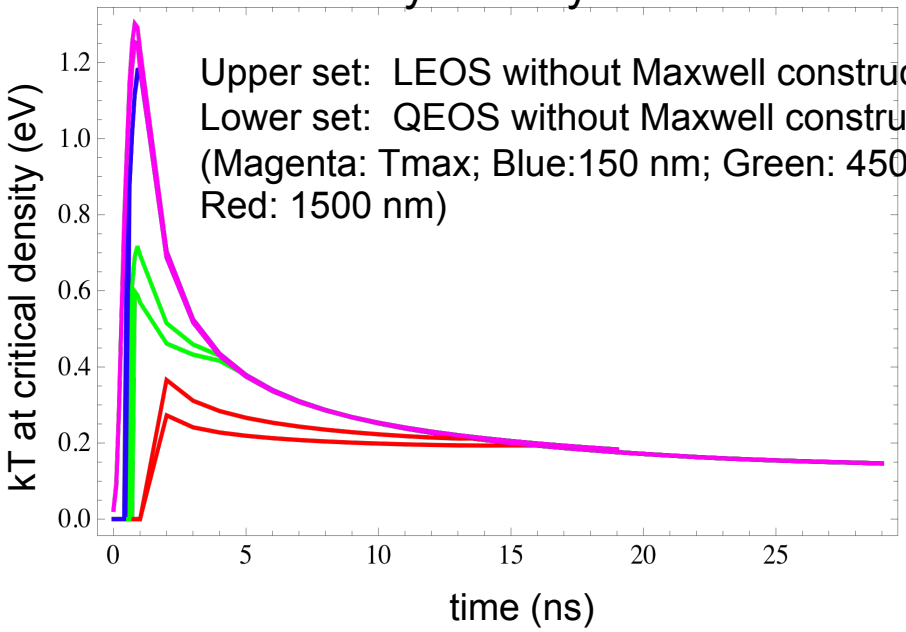

VISAR

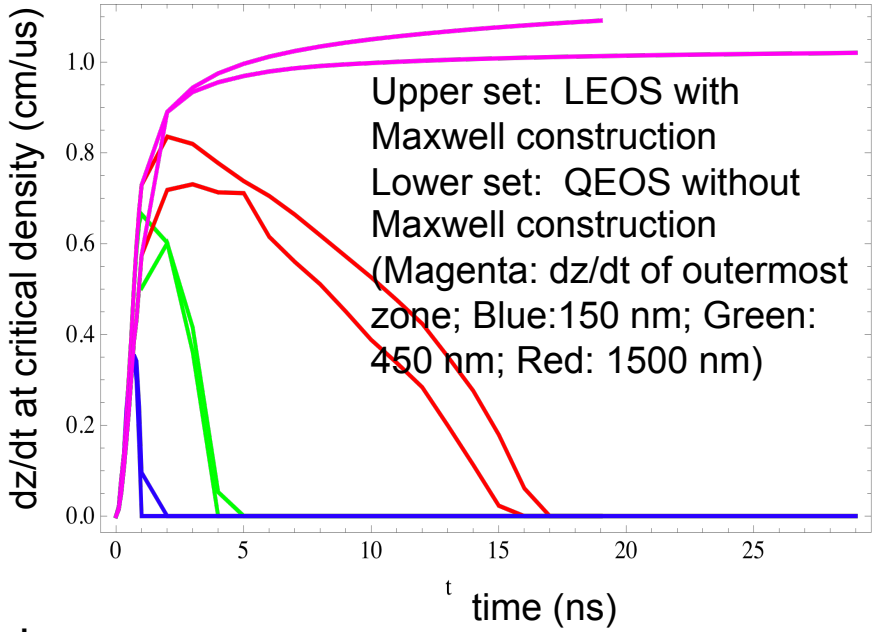

Multi-frequency (upper left) and multi-angle pyrometry measurements, together with multi-frequency Visar measurements (upper right) can also distinguish between candidate EOSs.

X-pinch

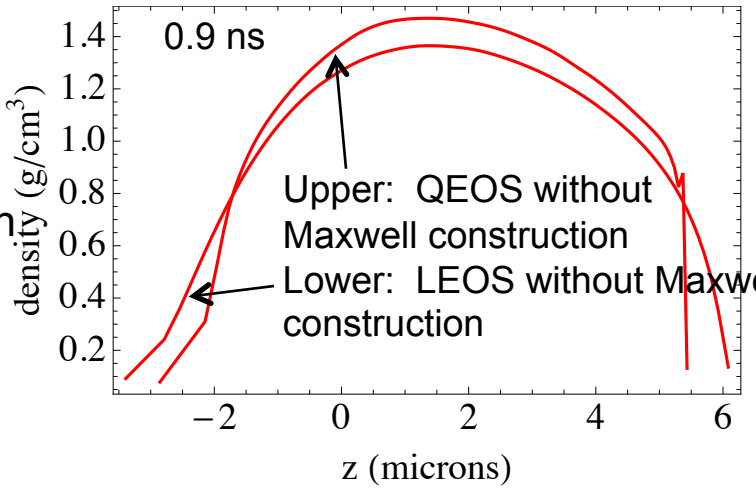

X-ray imaging of density profile (lower) can distinguish between EOS and for "instantaneous" heating and in simple wave regime can measure $c_s(\rho)$ and $P(\rho)$ directly (Foord et al Rev Sci Inst. (2004)).

At 1.2 MeV ion energy, with same target there is less uniformity and lower pressure

Assumed fluence:
8.4 J/cm^2; 1.2 MeV
Li beam on Al
target (0.85 ns)

density

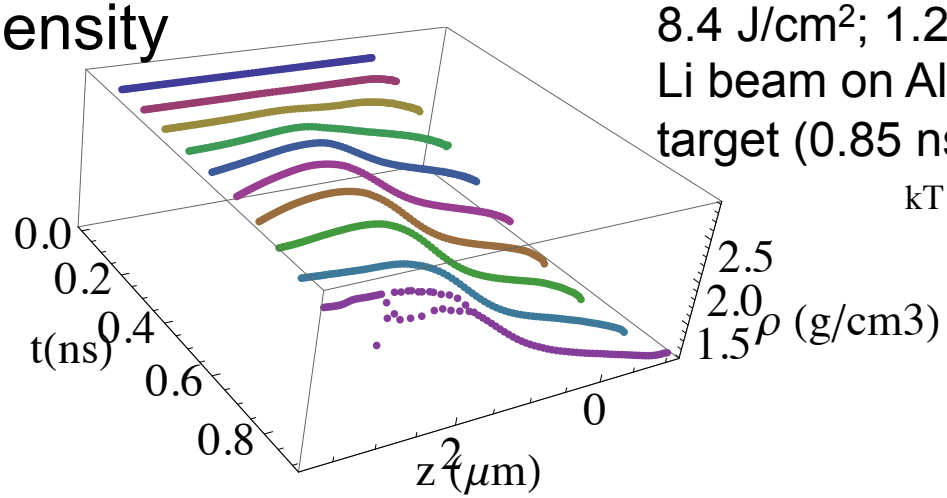

temperature

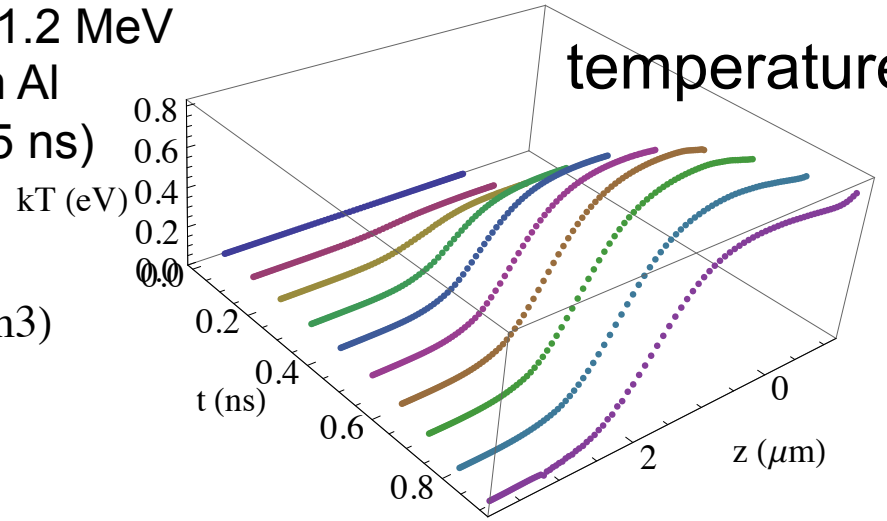

pressure

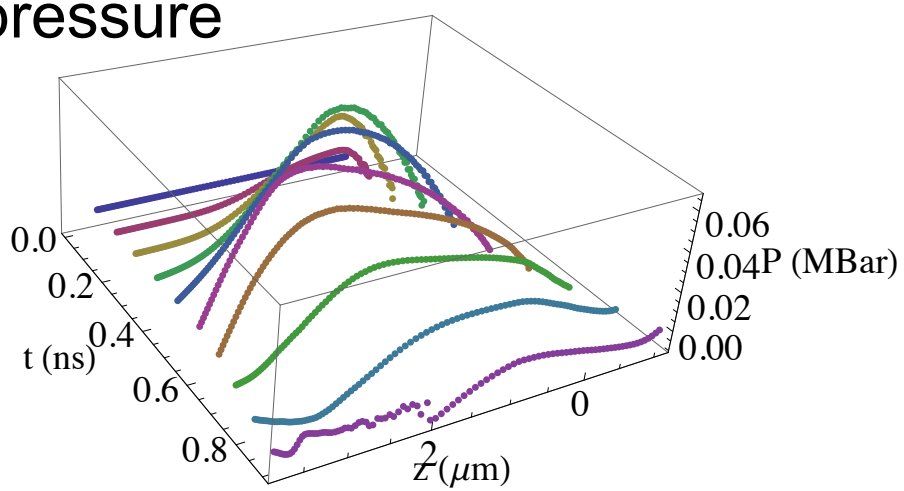

temp vs. density trajectories

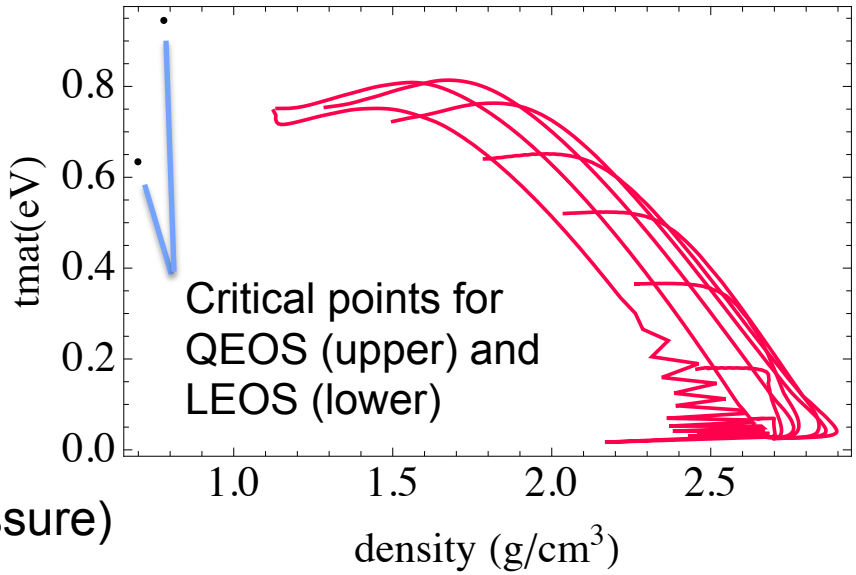

(Here foil thickness > ion range – maximizes pressure)

At 1.2 MeV ion energy, with target sub-range (1 μ) there is more uniformity at lower pressure,

Assumed fluence:
8.4 J/cm^2; 1.2 MeV
Li beam on Al
target (0.85 ns)

density

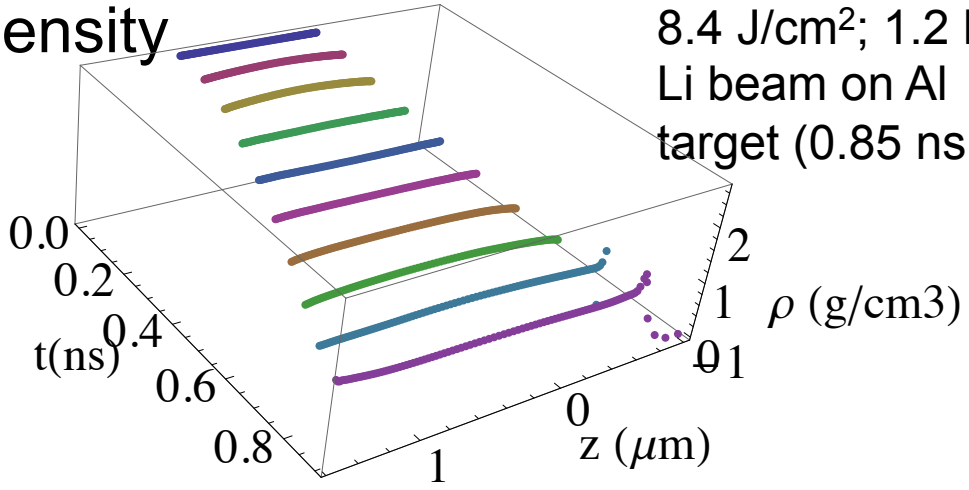

temperature

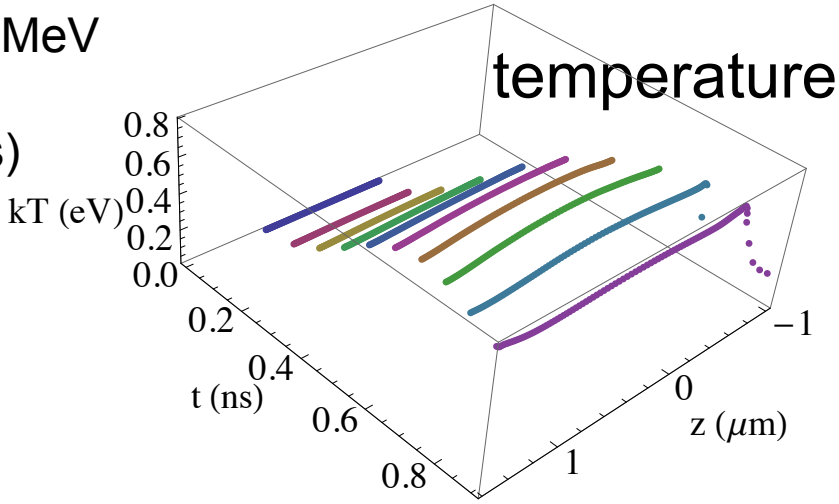

pressure

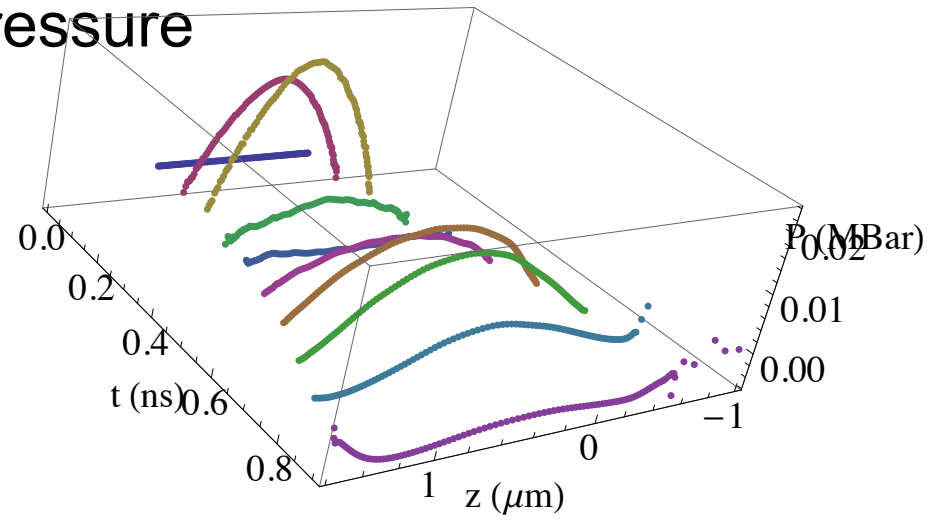

temp vs. density trajectories

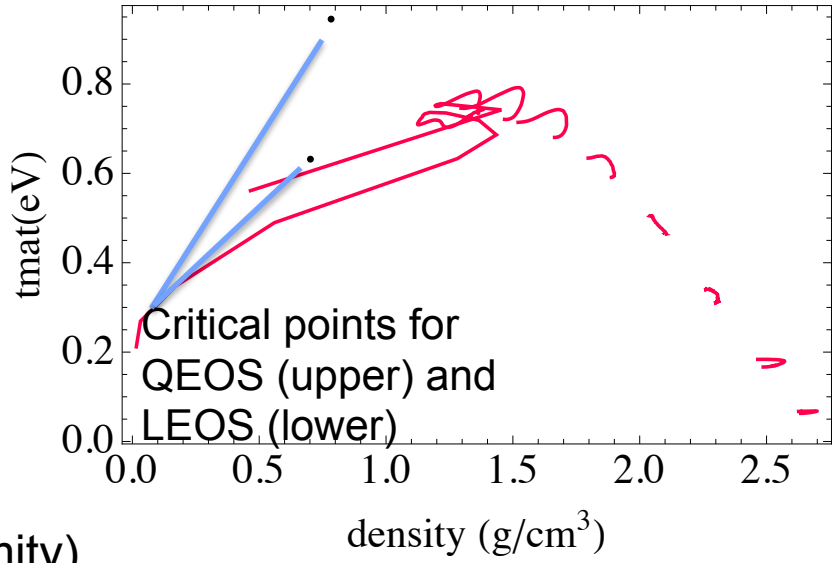

(Here foil thickness < ion range – for better uniformity)

HYDRA simulations of NDCX-II beams incident on Al foams show the formation of shocks and the effect of ion energy ramp

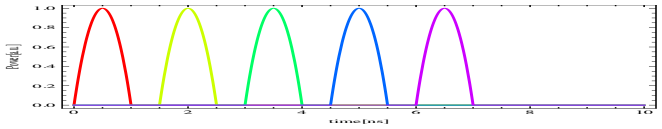

6 ns "macro-pulse"

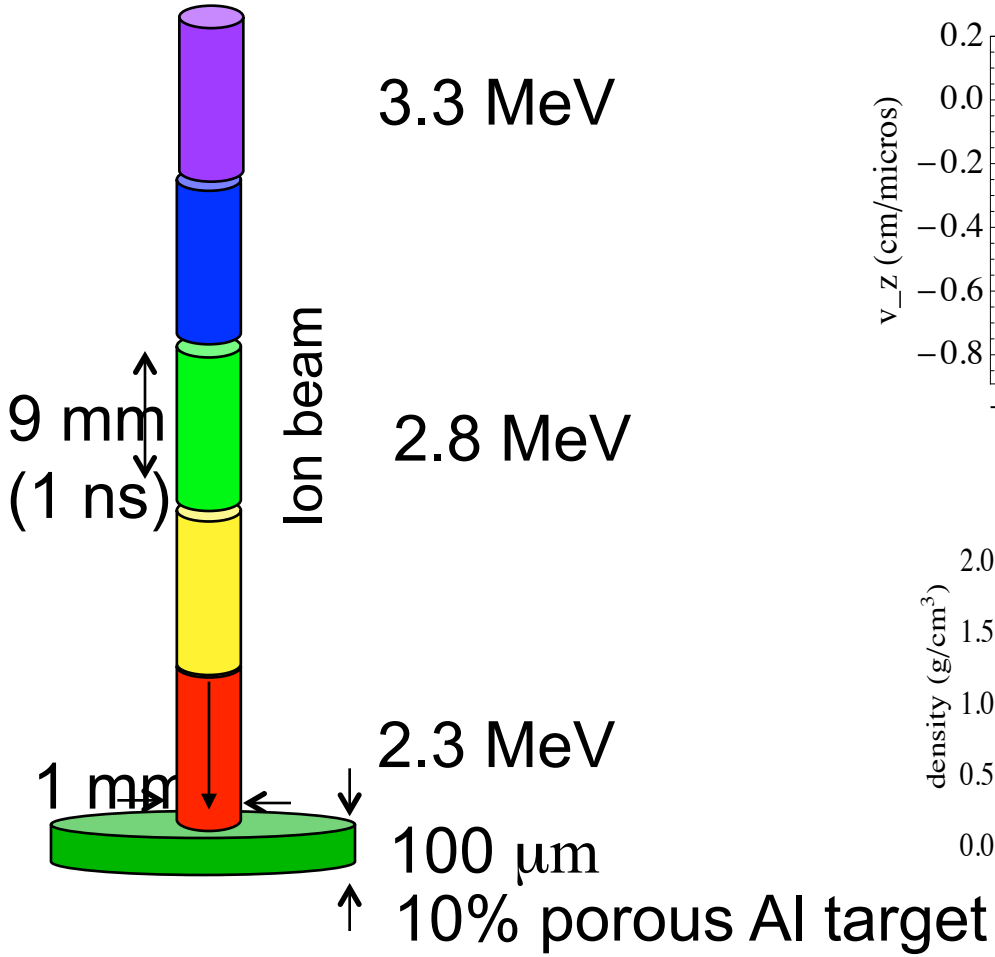

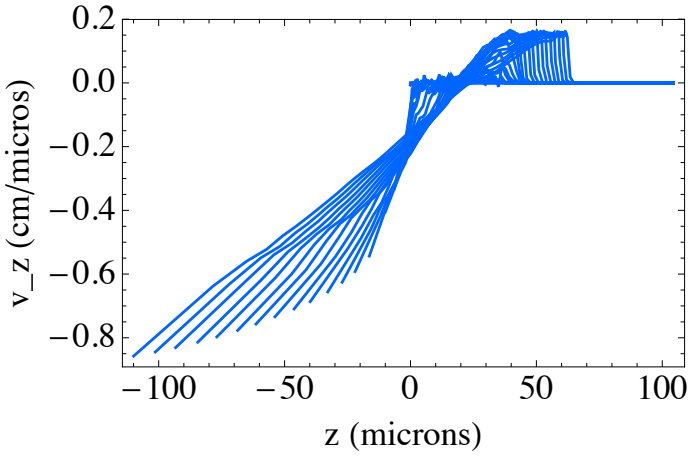

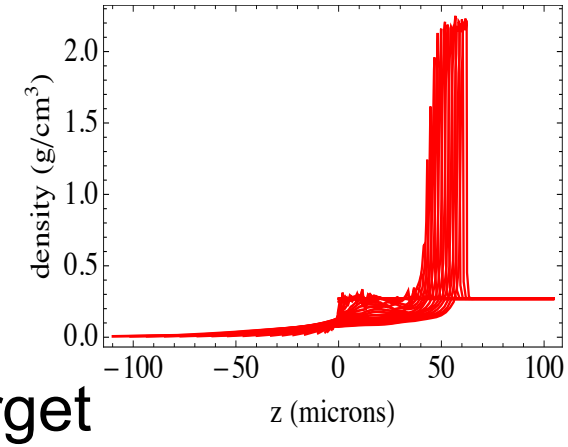

Shock positions at 18 and 20 ns illustrate the "sweet spot" at optimal slew rate

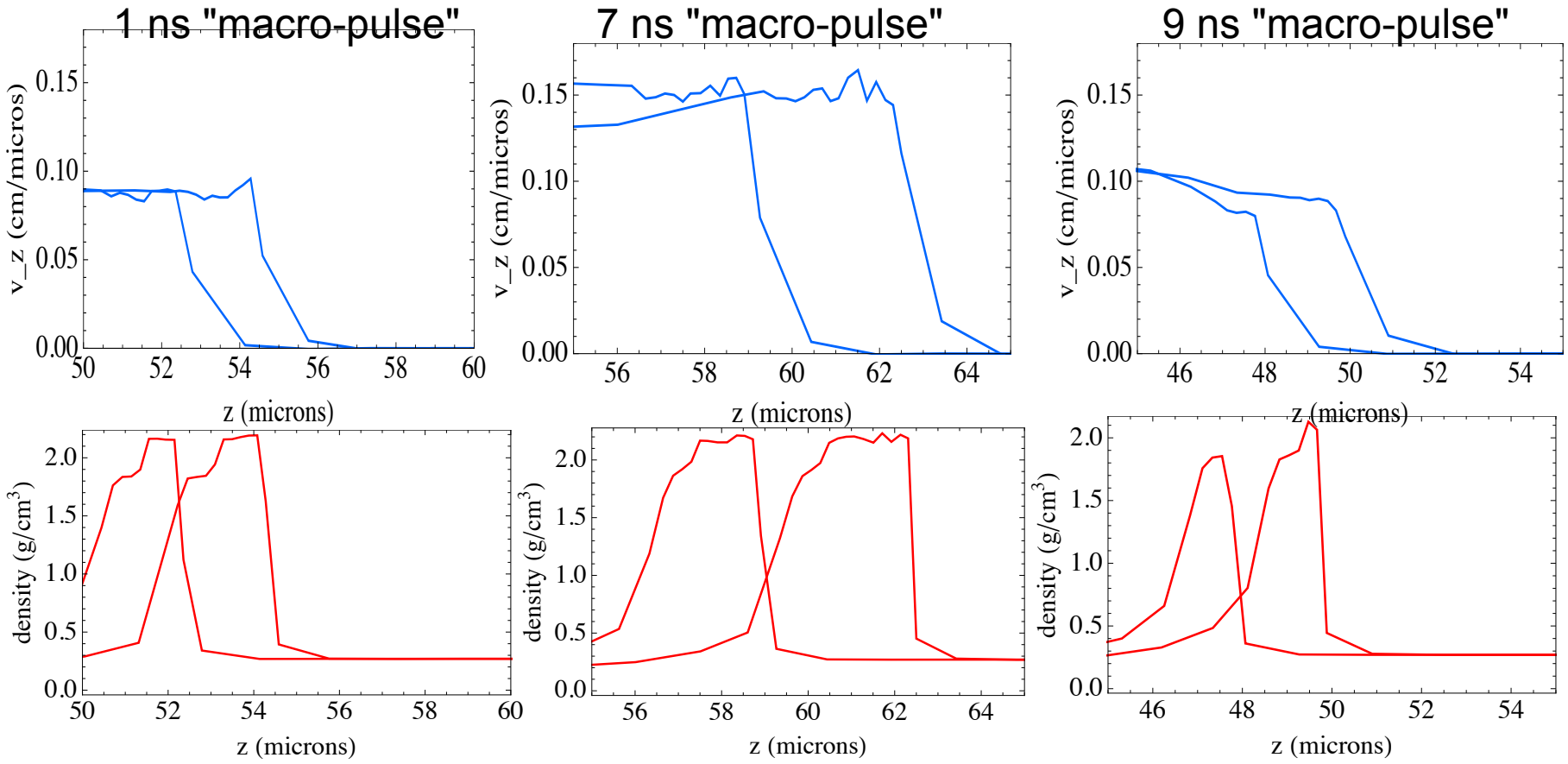

	1 ns "macro-pulse"	7 ns "macro-pulse"	9 ns "macro-pulse"
V_shock =	1.0 μ/ns	1.8 μ/ns	1.0 μ/ns
V_fluid =	0.9 μ/ns	1.6 μ/ns	0.9 μ/ns
ρ_fluid =	2.2 g/cm^3	2.2 g/cm^3	2.2 g/cm^3

Shock positions at 18 and 20 ns illustrate the "sweet spot" at optimal slew rate

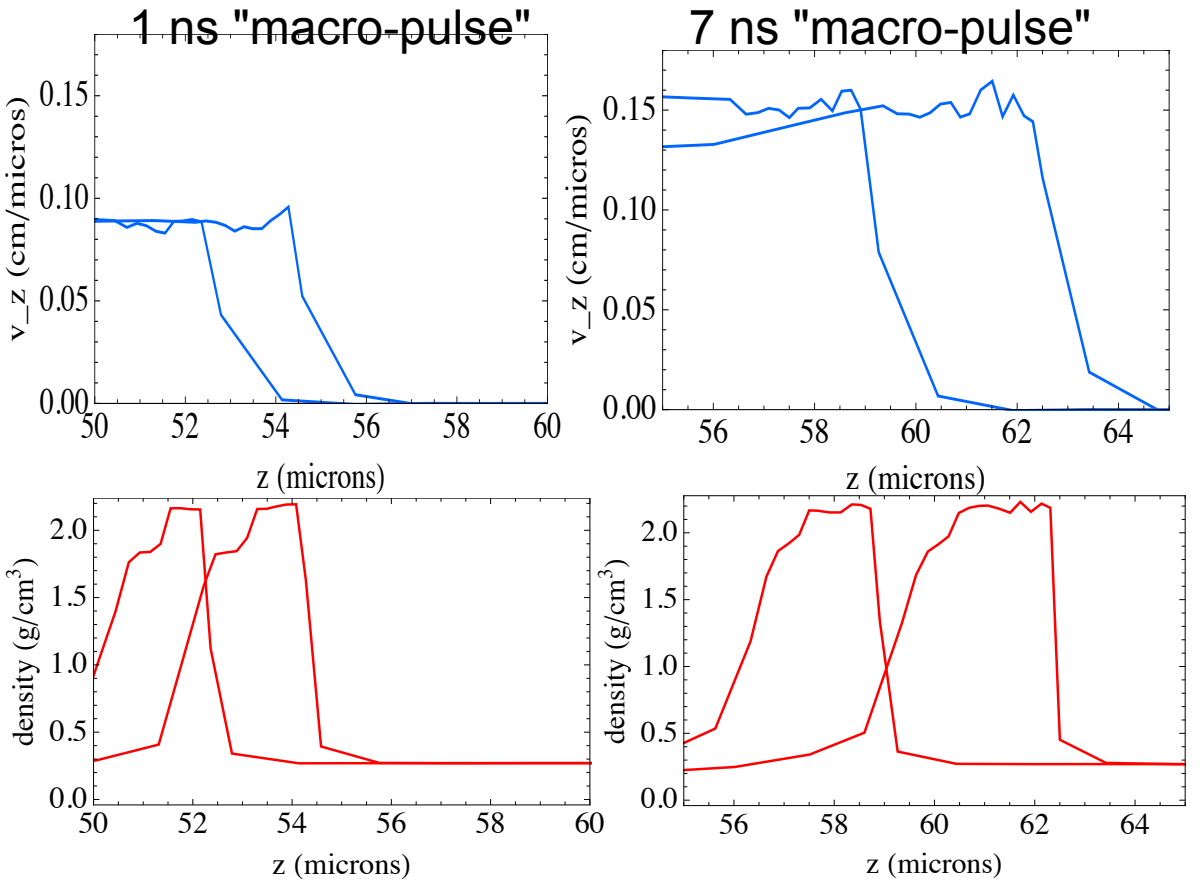

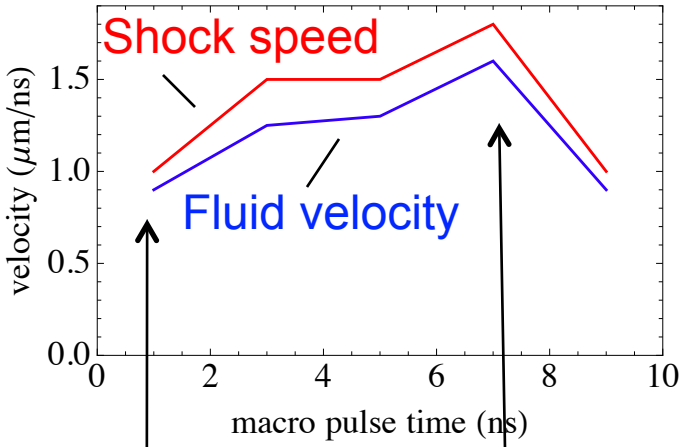

At longitudinal focus

At optimal slew rate

V_shock =	1.0 μ/ns	1.8 μ/ns
V_fluid =	0.9 μ/ns	1.6 μ/ns
ρ_fluid =	2.2 g/cm^3	2.2 g/cm^3

Shock strength depends on energy profile but also depends on intensity profile (and thus on how the beam focused in z, r)

Shock strength maximization with ion beams involves determining optimum velocity tilt and focusing angle:

Large velocity tilt gives:

larger range variation (larger variation in penetration depth)
shorter pulse duration
larger chromatic variations (*i.e.* larger spot radii at high velocity ends)

Large focusing angle:

smaller radius for midpulse of beam
larger chromatic variations (*i.e.* larger spot radii at high velocity ends)

For WDM (shockless) applications, requirements of short pulse and maximum energy density lead to large velocity tilt and optimum focusing angle

For IFE applications that create a shock, placing energy behind shock implies optimum may shift to longer pulses and smaller focusing angles

Tampers (that can be used in HI direct drive targets) can create additional shocks that can merge with the primary (M. Terry)

NDCX-II experimental scenario:

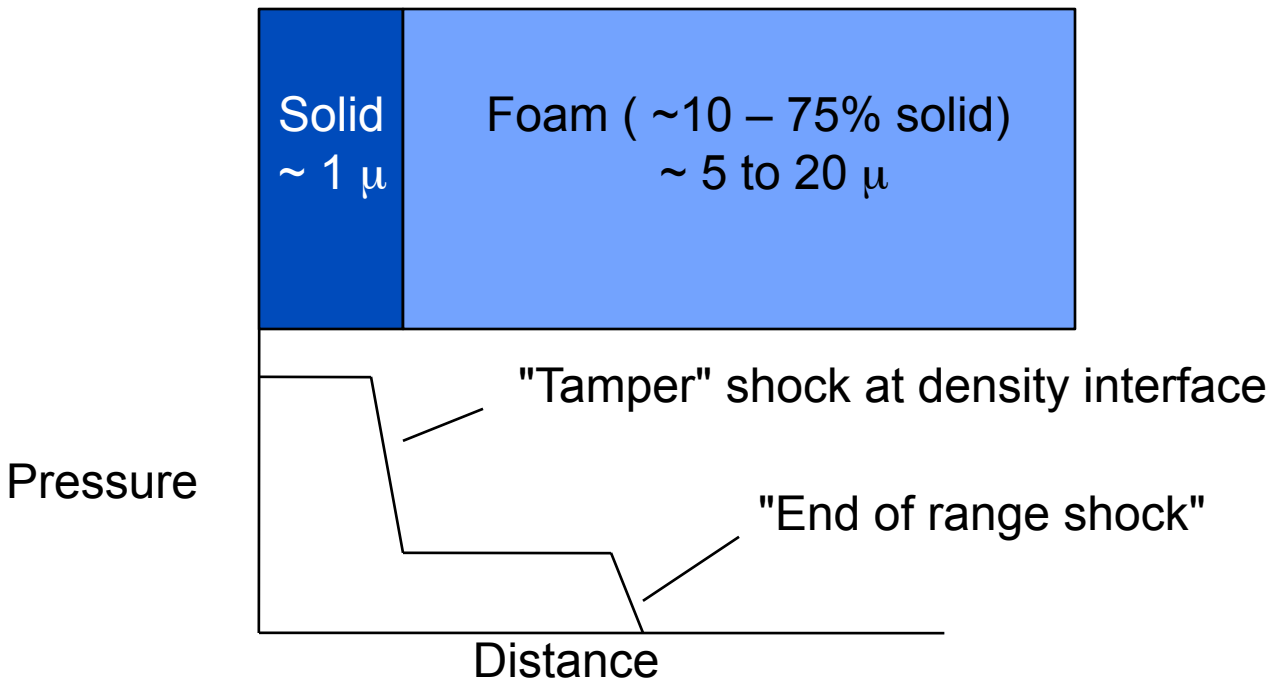

"Tamper shock" can catch up with "end of range shock"

Tamper absorbs energy that is not necessarily converted to mass flow.

What is the optimal combination of tamper thickness, density for efficient conversion to flow kinetic energy?

Effects of tamping, including optimal density profile of tamper, can be explored on NDCX-II

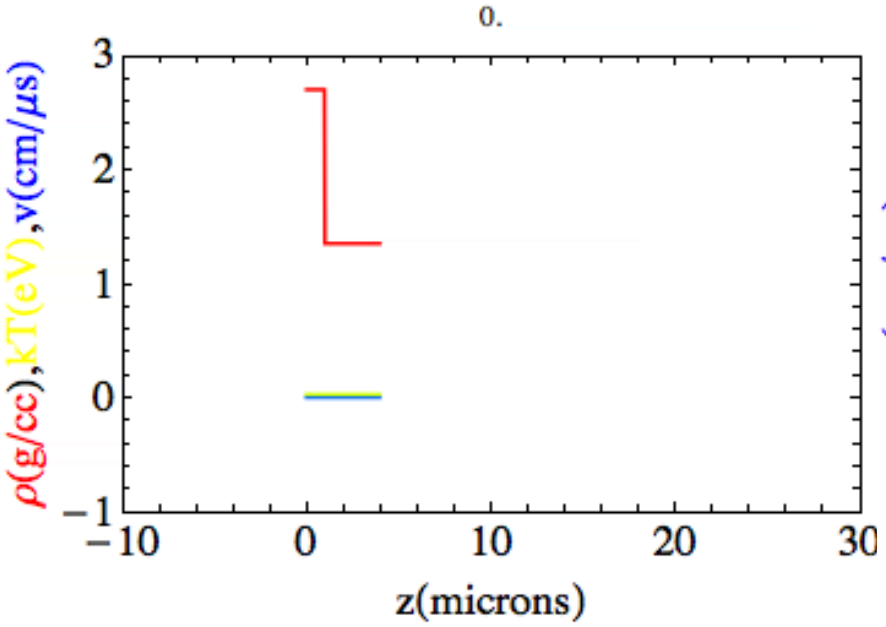

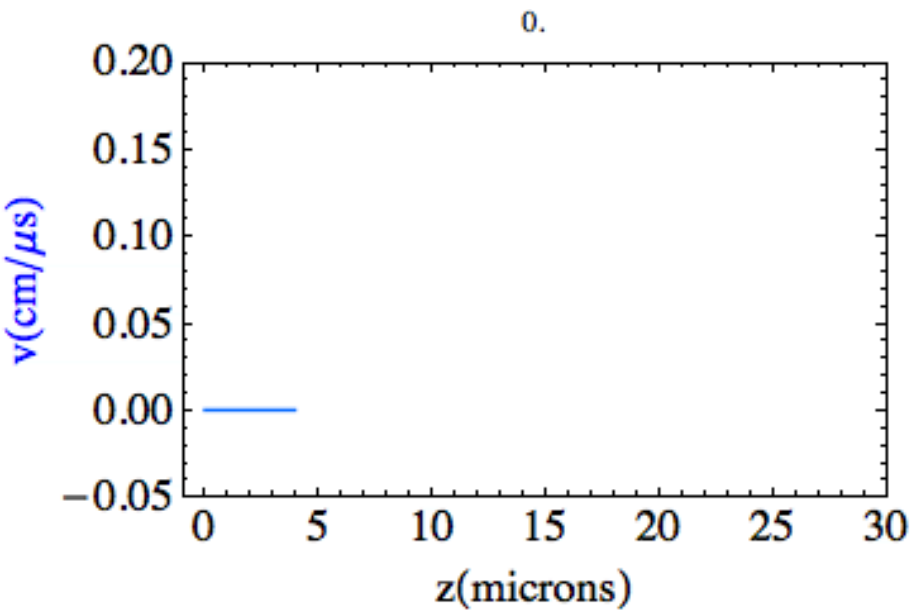

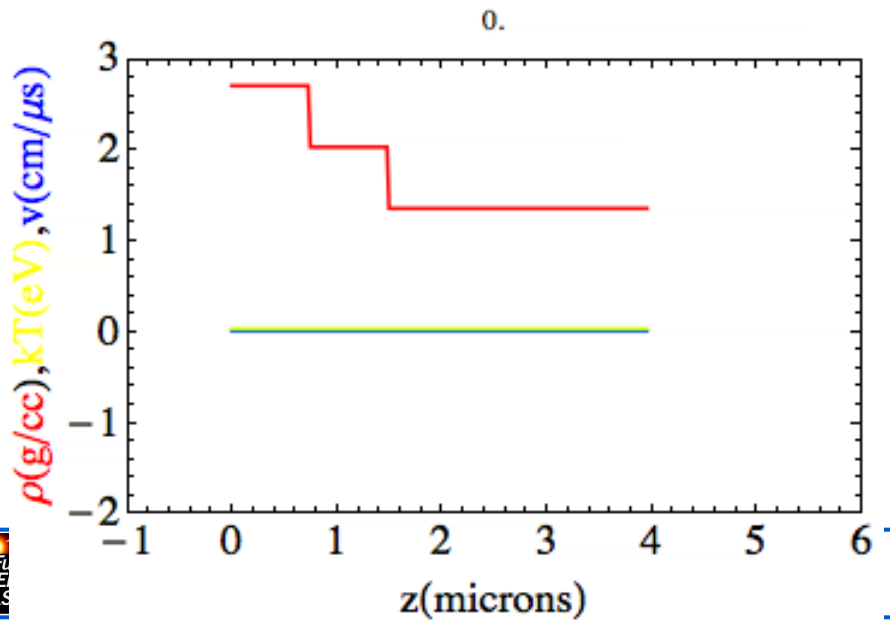

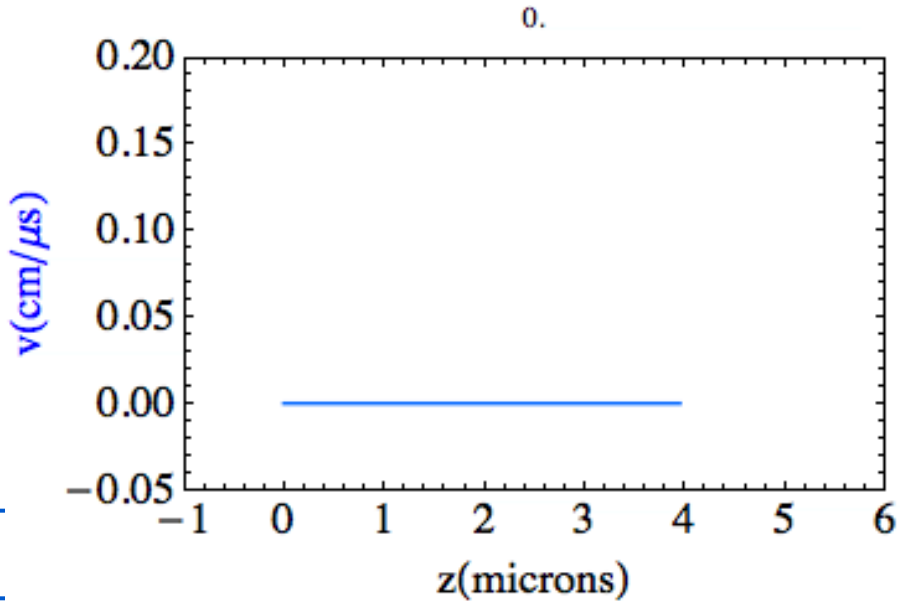

Types of measurement and diagnostics to obtain physical data on the material state

1. Time dependent measurement of rarefaction waves and hydrodynamic expansion of the heated material. This includes measurements of:
    a. temperature at the critical density by photometry of the emission as a function of wavelength, emission angle, and polarization (polarization pyrometry);
    b. velocity at the critical density (Visar); and
    c . density as a function of position, by measurement of absorbed X-rays created by an X-pinch or laser produced X-ray source.
2. Measurement of shock wave velocities, by imaging and timing of the breakout of the shockwave, and by measuring fluid velocities at the breakout time using VISAR, for those configurations in which shock waves are generated.
3. Electrical and thermal conductivity measurements, by measuring thermal breakout times of thin foils of various thicknesses, and B-field penetration times through heated matter.
4. Measurement of the final charge state and energy of the ions after passing through the target. One can measure both total energy of the beam to determine the deposition and also the energy of the ions to ensure that the deposition mechanisms are understood.
5. Measurement of emission and absorption spectral lines of the heated target for investigation of atomic physics in the Warm Dense Matter regime.
6. Aerogel witness media to capture droplets and fragments from the exploding media.
7. Laser probe measurements to optically measure target light transmission, reflection and absorption.

Ion stopping rates (dE/dX) in heated matter can be measured using NDCX-II both directly and indirectly

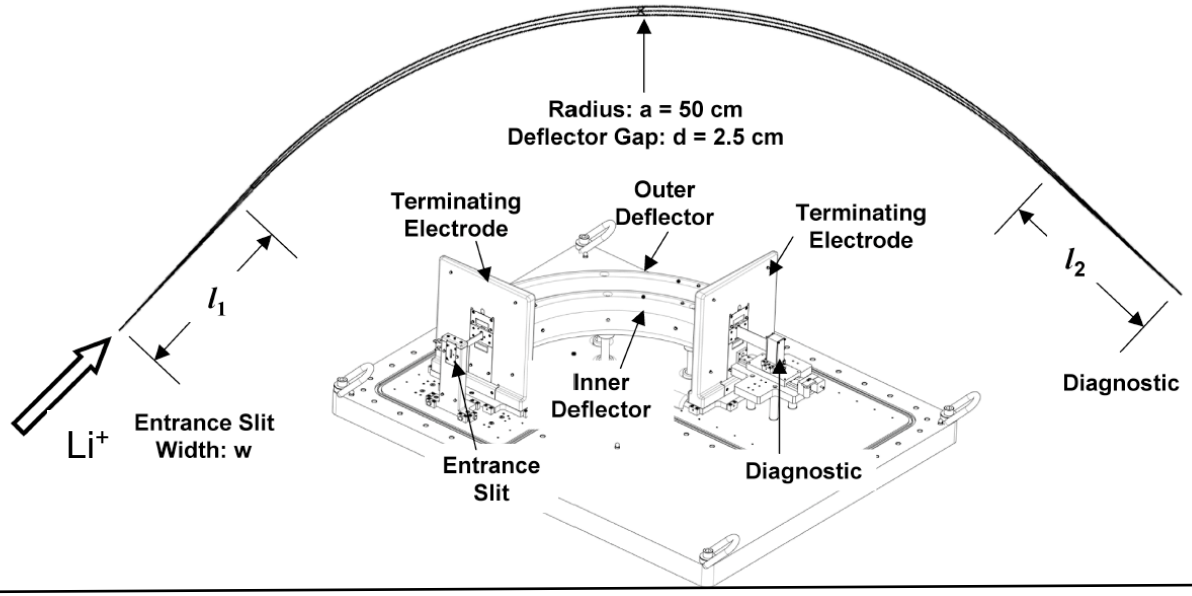

We are evaluating electrostatic energy analyzer (EEA) or other direct energy diagnostic for use on NDCX-II . Space issue main concern for EEA.

Indirect method (R. More): measure neutron production on deuterated carbon (plastic CD_2) target or (better) targets with known fraction of D and T.

Li+ + D → "knock-on" D (~100 kV) + D → n + charged particles

Number of created neutrons proportional to $1/(dE/dX|_{Li}) \times 1/(dE/dX|_{D})$ since the lower the dE/dX the greater chance a knock on collision will occur and the greater chance a neutron producing reaction can occur.

Polarization pyrometry: extra information is contained in polarization of emitted light

- Emission of *p* and *s* components of thermal light at angle, α and wavelength λ:

$$I_p^{\alpha}(\lambda) = \left(1 - \left|\frac{\xi(n,k)\cdot\cos(\alpha) - \sqrt{\xi(n,k) - \sin^2(\alpha)}}{\xi\cdot\cos(\alpha) + \sqrt{\xi - \sin^2(\alpha)}}\right|^2\right) \times \frac{C_1}{\lambda^5}\frac{1}{e^{\frac{C_2}{\lambda T}} - 1},$$

$$I_s^{\alpha}(\lambda) = \left(1 - \left|\frac{\cos(\alpha) - \sqrt{\xi(n,k) - \sin^2(\alpha)}}{\cos(\alpha) + \sqrt{\xi(n,k) - \sin^2(\alpha)}}\right|^2\right) \times \frac{C_1}{\lambda^5}\frac{1}{e^{\frac{C_2}{\lambda T}} - 1},$$

$$\xi = (n - ik)^2 - \text{complex dielectric function.}$$

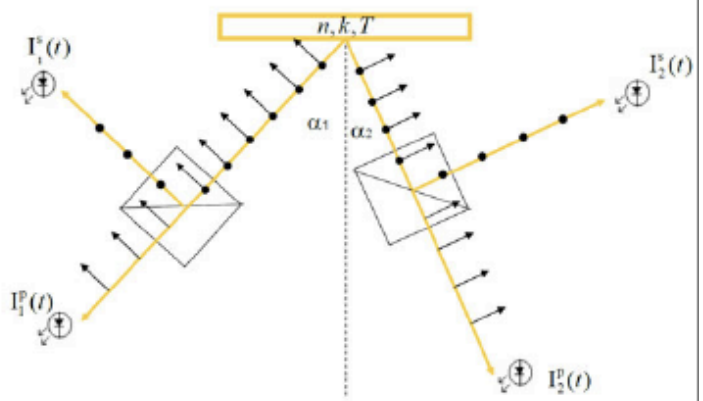

- If the absolute intensities of polarization components at two angles (four values in total) are measured, there is a **UNIQUE solution** for *T*, *n* and *k* (or ε).

- One can take data at more angles and obtain an over-determined system of equations, which is favorable when measurements have finite accuracy.

Other areas of interest to investigators of WDM, IFE, and HIFS that may be explored in NDCX-II

1. Phase transitions: in particular liquid-vapor phase transition and the complete boundary between the regions, and critical points. (Critical point is poorly known for many of the refractory metals). (Solid-liquid phase transitions is also of interest for some material.)

2. Phase transitions from metal to insulator and insulator to metal.

3. Transitions in opacity: (for example, the transition between transparent and opaque, as in transient darkening)

4. Fragmentation/fracture mechanics of materials under extreme conditions (e.g. carbon, silicon)

5. Droplet formation and the role of surface tension in rapidly expanding metals

6. In addition to ion beam stopping, scattering, and charge state evolution in WDM targets

7. Unusual plasma configurations, such as positive/negative plasmas (with low concentrations of electrons) as in halogens and some metals such as gold and platinum at temperatures above 0.4 eV.

Conclusions

1. NDCX-II will allow investigations of:
   - Heavy ion fusion beam physics
   - Warm dense matter target physics
   - IFE relevant target physics

2. At 1.2 MeV we will begin to study ion beam coupling, including study of rarefaction waves to distinguish EOS models, ion based shock optimization and tamped shock physics, dE/dX measurements, and conductivity measurements

3. At ~3 MeV additional WDM/IFE target experiments are possible:

   Ion energy exceeds Bragg peak in more material, increasing homogeneity; ion range longer, increasing hydro time; emittance scaling allows brighter beams, increasing target energy density